Inorganica Chimica Acta, *145* (1988) 195–203

Oligophosphine Ligands.
XXVI*. Halogenomolybdenum Complexes Containing Oligo(tertiary) Phosphine Ligands: Synthesis, Electrochemistry, and Molecular Structures

B. PIETSCH and L. DAHLENBURG**

Institut für Anorganische und Angewandte Chemie der Universität Hamburg, Martin-Luther-King-Platz 6, D-2000 Hamburg 13, F.R.G.

(Received August 26, 1987)

Abstract

The reaction of $MoCl_3(OC_4H_8)_3$ with $MeP(CH_2CH_2CH_2PMe_2)_2$ in THF gave the unsolvated complex $MoCl_3[MeP(CH_2CH_2CH_2PMe_2)_2]$ (2) as well as its addition compound $2 \cdot 0.75OC_4H_8$, which are analogues of the previously reported $MoCl_3[PhP(CH_2CH_2CH_2PPh_2)_2]$ (1). Sodium amalgam reduction of $2 \cdot 0.75OC_4H_8$ in the presence of PMe_3 or PMe_2Ph, in THF under nitrogen atmosphere, yielded the Mo(II) derivatives $MoCl_2[MeP(CH_2CH_2CH_2PMe_2)_2](PMe_3)$ (3) and $MoCl_2[MeP(CH_2CH_2CH_2PMe_2)_2](PMe_2Ph)$ (4). The electrochemical investigation of complexes 1 and 2 (performed on THF solutions of the addition compounds $1 \cdot CH_2Cl_2$ and $2 \cdot 0.75OC_4H_8$ by cyclic voltammetry) demonstrated that the reduction products 2^- and 3^- undergo rapid replacement of chloride by solvent and phosphine donor molecules. Whereas 2^- and its Cl^-/PMe_3 substitution product were not reduced further at potentials > *ca.* −2.50 V (*versus* $Ag/AgNO_3$, 0.1 M, in CH_3CN), the voltammogram of 1 revealed a further reduction step occurring at −2.40 V in the presence of added PPh_2Me. This is consistent with the finding that 1, but not 2, is easily reduced to low valent molybdenum complexes by chemical reductants, such as sodium amalgam. X-ray crystallography established a meridional-octahedral arrangement of the ligands for complexes 1 and 2, and a *trans*-octahedral coordination geometry for compounds 3 and 4. Relevant crystallographic data are: $1 \cdot CH_2Cl_2$: orthorhombic *Pbca*, $a = 1677.5(9)$, $b = 3167(1)$, $c = 1457.9(9)$ pm, $Z = 8$, $R = 0.119$, $R_w = 0.116$ (1790 data). $2 \cdot 0.75OC_4H_8$: tetragonal $I\bar{4}$, $a = 1733.5(4)$, $c = 1589.7(5)$ pm, $Z = 8$, $R = 0.050$, $R_w = 0.041$ (1689 data). $3 \cdot 0.50CH_3OH$: orthorhombic $Pca2_1$, $a = 1491.1(12)$, $b = 1168.0(7)$, $c = 1434.1(9)$, $Z = 4$, $R = 0.071$, $R_w = 0.072$ (1380 data). 4: monoclinic $P\bar{1}$, $a = 1375.7(4)$, $b = 1892(1)$, $c = 2074(1)$ pm, $\alpha = 86.86(5)$, $\beta = 88.06(4)$, $\gamma = 84.81°$, $Z = 8$, $R = 0.085$, $R_w = 0.073$ (9284 data).

Introduction

In earlier publications [2, 3], we have reported that the reduction of $MoCl_3[PhP(CH_2CH_2CH_2PPh_2)_2]$ (1) with sodium amalgam in the presence of the monotertiary phosphines $PMe_{3-n}Ph_n$ ($n = 0, 1, 2$) in THF under nitrogen atmosphere, gives the bis(dinitrogen) complexes *trans*-$Mo(N_2)_2[PhP(CH_2CH_2CH_2PPh_2)_2](PMe_{3-n}Ph_n)$. In continuation of this work we became interested in examining the chemistry of some potentially electron-rich molybdenum complexes derived from the completely alkylated bis(chelate) phosphine $MeP(CH_2CH_2CH_2PMe_2)_2$ [4]. This interest was reinforced upon the recent publications of Carmona and Green and their co-workers demonstrating the ability of molybdenum complexes with electron-releasing phosphine ligands to activate even notoriously inert systems, such as carbon dioxide [5–7] and carbon–hydrogen bonds [8].

This paper deals with the preparation of the Mo(III) complex $MoCl_3[MeP(CH_2CH_2CH_2PMe_2)_2]$ (2) as well as with its chemical reduction to $MoCl_2[MeP(CH_2CH_2CH_2PMe_2)_2](PMe_3)$ (3) and $MoCl_2[MeP(CH_2CH_2CH_2PMe_2)_2](PMe_2Ph)$ (4). We also describe the electrochemical behaviour of compound 2 studied by cyclic voltammetry and compare it with that of its previously reported analogue 1. Finally, we present the results of single-crystal X-ray studies performed on 1–4 with the objective of elucidating the hitherto unknown coordination geometry of these chelate phosphine molybdenum complexes.

Experimental

General Procedures

All reactions were carried out under nitrogen atmosphere using standard Schlenk techniques.

---

*For Part XXV, see ref. 1.

**Author to whom correspondence should be addressed.

0020-1693/88/$3.50

Solvent were dried according to recommended methods and were distilled under nitrogen prior to use.

Preparation of Complexes

$MoCl_3[PhP(CH_2CH_2CH_2PPh_2)_2]$ (1)

This compound was synthesized from $PhP(CH_2CH_2CH_2PPh_2)_2$ and $MoCl_3(OC_4H_8)_3$ as described previously [2].

$MoCl_3[MeP(CH_2CH_2CH_2PMe_2)_2]$ (2)

$MeP(CH_2CH_2CH_2PMe_2)_2$ (13.0 ml, *ca.* 48 mmol) [4] was added to a suspension of 19.0 g (45.4 mmol) of freshly prepared orange $MoCl_3(OC_4H_8)_3$ [9] in THF (270 ml). Stirring of this mixture at room temperature for 60 h caused the slow deposition of unsolvated $MoCl_3[MeP(CH_2CH_2CH_2PMe_2)_2]$ as a beige fine-grained precipitate which was separated by filtering, washed with THF (3 × 10 ml), and dried *in vacuo*. Yield: 6.1 g (30%). *Anal.* Found: C, 29.3; H, 6.1; Cl, 23.0; Mo, 20.2. Calc. for $C_{11}H_{27}Cl_3MoP_3$ (454.55): C, 29.07; H, 5.99; Cl, 23.40; Mo, 21.11%.

The reddish brown mother liquor of the above preparation was concentrated under reduced pressure to give a final volume of approximately 8 ml. Upon addition of 10 ml of diethyl ether the lattice compound $MoCl_3[MeP(CH_2CH_2CH_2PMe_2)_2]\cdot0.75OC_4H_8$ formed as canary yellow crystals which were collected by filtration, washed with Et_2O (5 ml) and hexane (2 × 10 ml) and dried under vacuum. Yield: 12.3 g (53%). *Anal.* Found: C, 32.6; H, 6.6; Cl, 21.2; Mo, 19.1. Calc. for $C_{14}H_{33}Cl_3MoO_{0.75}P_3$ (508.64): C, 33.06; H, 6.54; Cl, 20.91; Mo, 18.86%.

$MoCl_2[MeP(CH_2CH_2CH_2PMe_2)_2](PMe_3)$ (3)

The solution of 1.36 g (2.67 mmol) of $2\cdot0.75OC_4H_8$ and 0.32 ml of PMe_3 (*ca.* 3 mmol) in 75 ml of THF was mixed with 77.6 g of 0.8% sodium amalgam (equivalent to *ca.* 27 mmol Na) and vigorously stirred at room temperature for 60 h. The solution was then decanted from the alloy, filtered over silica gel, and evaporated to dryness. Dissolution of the residue in toluene (50 ml), followed by filtration and removal of the solvent under reduced pressure gave 0.39 g (30%) of yellow complex **3**. *Anal.* Found (after washing with hexane and drying *in vacuo*): C, 33.2; H, 7.4; Cl, 13.1. Calc. for $C_{14}H_{36}Cl_2MoP_4$ (495.18): C, 33.96; H, 7.33; Cl, 14.32%.

$MoCl_2[MeP(CH_2CH_2CH_2PMe_2)_2](PMe_2Ph)$ (4)

A sample of 1.50 g (2.95 mmol) of $2\cdot0.75OC_4H_8$ was dissolved in 100 ml of THF containing 0.46 ml of PMe_2Ph (*ca.* 3.5 mmol). Dilute sodium amalgam (65 g containing *ca.* 0.7%, *i.e.* 20 mmol Na) was then added, and the mixture was stirred vigorously at room temperature for 16 h. The excess amalgam was removed by decantation, and the THF solution was filtered over silica gel and evaporated to dryness. After redissolving the residue in toluene (40 ml), the filtration over silica was repeated until a clear filtrate was obtained. This was reduced in volume to approximately 2 ml. Upon addition of 5 ml of hexane, crystallization of complex **4** was induced by cooling to −78 °C. The gold-coloured crystals were collected by filtering, washed with cold hexane (2 × 5 ml) and dried *in vacuo*. The yield was 0.83 g (50%). *Anal.* Found: C, 40.8; H, 7.0; Cl, 12.9; Mo, 17.3. Calc. for $C_{19}H_{38}Cl_2MoP_4$ (557.26): C, 40.95; H, 6.87; Cl, 12.72; Mo, 17.22%.

Cyclic Voltammetric Measurements

The electrochemical investigations were performed on *ca.* 10^{-3} M solutions of the complexes in carefully purified and Al_2O_3 dried THF. Platinum wire was used as the working electrode. The reference electrode consisted of an Ag wire contacted with 0.1 M $AgNO_3$ in acetonitrile. $[n\text{-}Bu_4N]PF_6$, 0.1 M, was employed as the supporting electrolyte. Typical sweep rates were in the range 50–500 mV/s.

X-ray Studies

Crystals suitable for X-ray work grew from CH_2Cl_2/hexane (complex **1**), tetrahydrofuran (complex **2**), methanol (complex **3**) and toluene (complex **4**), respectively. Complexes **1**–**3** were obtained as addition compounds containing solvent of crystallization, *viz.* $1\cdot CH_2Cl_2$, $2\cdot0.75C_4H_8O$, and $3\cdot0.5CH_3OH$; complex **4** crystallized in an unsolvated form.

X-ray measurements were carried out at 20 °C on a Syntex P2$_1$ diffractometer using Mo Kα radiation ($\lambda = 71.069$ pm). For each structure, the orientation matrix and the final unit cell parameters were calculated by least-squares from the setting angles of 15 machine-centered reflections having $11° < 2\theta < 24°$. Diffraction intensities were measured by the $\theta/2\theta$ scan technique with variable scan rates (2.0°/min–29.3°/min) determined from a fast pre-scan on each reflection. No significant decrease was observed in the intensities of three standard reflections monitored periodically during data collection. Data were corrected for Lorentz and polarization effects, but not for absorption or extinction.

In each structure, the molybdenum as well as several of the chlorine and phosphorus atoms were readily located by comparison of the Patterson map with the results of the TREF direct-methods attempts of SHELXS-84 [10]. Subsequent alternate cycles of difference Fourier synthesis and least-squares refinement (full-matrix for compounds **1**–**3**, block-diagonal for complex **4**) using the SHELX-76 program package with scattering factors from the sources given therein [11] revealed the positions of the remaining non-hydrogen atoms.

For the refinement of structure **1**, a mixed thermal model assigning anisotropic behaviour to the metal, chlorine, and phosphorus atoms was adopted. Hydrogen positions remained unconsidered. The phenyl groups of the phosphine ligand and the solvent molecule were treated as rigid groups with C–C and C–Cl bond lengths fixed at 139.5 and 177.0 pm, respectively. The structural model resulting for compound 2 was refined with allowance for anisotropic thermal motion of all non-hydrogen atoms of the complex molecule. In this case, the hydrogen atoms of the chelate phosphine were included in the molecular model in geometrically idealized positions with C–H distances constrained to 96.0 pm. The THF molecules of crystallization were detected in positions consistent with their occurrence, *i.e.* near the axes 2 (4 molecules) and $\bar{4}$ (2 molecules) of a tetragonal $I\bar{4}$ cell containing 8 molecules of complex 2. In keeping with these positions, the ring atoms (which were treated isotropically) were found to display a heavy orientational disorder that could only partially be resolved. The final model of structure 3 also used anisotropic temperature factors for the non-hydrogen atoms of the complex, isotropic thermal parameters for the methanol C and O atoms, and calculated positions for the hydrogen atoms of the phosphine ligands. In the structural model of complex 4, which was anisotropically refined to convergence, hydrogen atoms were not included.

A summary of relevant crystallographic information and results is collected in Table I. Final positional parameters are presented in Tables II–V. Selected bond lengths and angles are given in the captions to Figs. 2–5 (see below) showing SCHAKAL-drawn perspective views of the molecules [12]. See also 'Supplementary Material'.

Results and Discussion

Preparative Findings

In earlier work [2], we obtained the compound $MoCl_3[PhP(CH_2CH_2CH_2PPh_2)_2]\cdot CH_2Cl_2$ ($1\cdot CH_2Cl_2$) by reaction of freshly prepared $MoCl_3(OC_4H_8)_3$ with one equivalent of the chelate phosphine in CH_2Cl_2/THF. Upon stirring $MoCl_3(OC_4H_8)_3$ with $MeP(CH_2CH_2CH_2PMe_2)_2$ in tetrahydrofuran, a beige precipitate analyzing as $MoCl_3[MeP(CH_2CH_2CH_2PMe_2)_2]$ (2) was gradually deposited. On account of its insolubility, this material has not been characterized further. Concentration of the mother liquor of 2 gave moderate yields of a soluble modification of the complex as canary yellow crystals, which were identified as the addition compound $MoCl_3(MeP(CH_2CH_2CH_2PMe_2)_2]\cdot 0.75OC_4H_8$ ($2\cdot 0.75OC_4H_8$) by elemental analysis and X-ray diffraction (*vide infra*).

During attempts to prepare dinitrogen derivatives of the series $Mo(N_2)_2[MeP(CH_2CH_2CH_2PMe_2)_2](PR_3)$ under reductive conditions that had previously been shown to be suitable for the $PhP(CH_2CH_2CH_2PPh_2)_2$ analogues $Mo(N_2)_2[PhP(CH_2CH_2CH_2PPh_2)_2](PR_3)$ [2], we found that the sodium amalgam

TABLE I. Crystallographic Data

	$1\cdot CH_2Cl_2$	$2\cdot 0.75C_4H_8O$	$3\cdot 0.5CH_3OH$	4
M	849.85	508.64	511.21	557.26
Crystal system	orthorhom.	tetragonal	orthorhom.	triclinic
Space group	*Pbca*	$I\bar{4}$	$Pca2_1$	$P\bar{1}$
a (pm)	1677.5(9)	1733.5(4)	1491.1(12)	1375.7(4)
b (pm)	3167(1)	1733.5(4)	1168.0(7)	1892(1)
c (pm)	1457.9(9)	1589.7(5)	1434.1(9)	2074(1)
α (°)	90	90	90	86.86(5)
β (°)	90	90	90	88.06(4)
γ (°)	90	90	90	84.81(4)
V (× 10^6 pm^3)	7745	4777	2498	5366
Z	8	8	4	8
D (g/cm^3)	1.46	1.41	1.36	1.38
μ (Mo Kα) (cm^{-1})	7.5	9.9	9.0	8.4
Max. 2θ (deg)	40	50	50	45
Number of data				
collected	8009	3094	2509	14858
independent	3651	2348	2293	14144
used ($F_o > 4\sigma$)	1790	1689	1380	9284
Number of parameters refined	167	197	204	940
Data/parameters	10.7	8.6	6.8	9.9
R	0.119	0.050	0.071	0.085
R_w	0.116[a]	0.041[b]	0.072[c]	0.073[d]

[a] $w = 1/(\sigma^2(F_o) + 0.001(F_o)^2)$. [b] $w = 1/(\sigma^2(F_o) + 0.0001(F_o)^2)$. [c] $w = 1$. [d] $w = 1/\sigma^2(F_o)$.

TABLE II. Positional Parameters of **1**·CH_2Cl_2

Atom[a]	x/a	y/b	z/c
Mo	0.2107(2)	0.1644(1)	0.1758(2)
Cl(1)	0.2944(6)	0.1903(3)	0.0512(6)
Cl(2)	0.1347(5)	0.1387(3)	0.3033(6)
Cl(3)	0.0948(5)	0.1902(3)	0.0997(6)
P(1)	0.2200(6)	0.0907(3)	0.0980(6)
P(2)	0.3446(6)	0.1468(3)	0.2458(6)
P(3)	0.2167(6)	0.2313(3)	0.2734(6)
C(1)	0.279(2)	0.220(1)	0.377(2)
C(2)	0.367(3)	0.221(2)	0.362(3)
C(3)	0.398(2)	0.196(1)	0.275(2)
C(4)	0.416(2)	0.123(1)	0.162(2)
C(5)	0.391(2)	0.076(1)	0.134(2)
C(6)	0.321(2)	0.076(1)	0.059(2)
C(7)	0.165(2)	0.083(1)	−0.010(2)
C(8)	0.136(2)	0.044(1)	−0.036(2)
C(9)	0.096(2)	0.039(1)	−0.119(2)
C(10)	0.084(2)	0.074(1)	−0.176(2)
C(11)	0.113(2)	0.113(1)	−0.150(2)
C(12)	0.154(2)	0.118(1)	−0.067(2)
C(13)	0.185(2)	0.046(1)	0.166(2)
C(14)	0.107(2)	0.047(1)	0.201(2)
C(15)	0.080(2)	0.015(1)	0.258(2)
C(16)	0.129(2)	−0.019(1)	0.280(2)
C(17)	0.207(2)	−0.020(1)	0.245(2)
C(18)	0.234(2)	0.012(1)	0.188(2)
C(19)	0.359(2)	0.114(1)	0.349(1)
C(20)	0.300(2)	0.086(1)	0.378(1)
C(21)	0.311(2)	0.062(1)	0.457(1)
C(22)	0.381(2)	0.067(1)	0.508(1)
C(23)	0.440(2)	0.095(1)	0.480(1)
C(24)	0.429(2)	0.119(1)	0.400(1)
C(25)	0.253(2)	0.282(1)	0.231(2)
C(26)	0.250(2)	0.292(1)	0.138(2)
C(27)	0.275(2)	0.331(1)	0.108(2)
C(28)	0.302(2)	0.361(1)	0.170(2)
C(29)	0.305(2)	0.351(1)	0.264(2)
C(30)	0.280(2)	0.312(1)	0.294(2)
C(31)	0.121(1)	0.247(1)	0.321(2)
C(32)	0.092(1)	0.232(1)	0.405(2)
C(33)	0.018(1)	0.245(1)	0.437(2)
C(34)	−0.028(1)	0.273(1)	0.386(2)
C(35)	0.001(1)	0.288(1)	0.303(2)
C(36)	0.075(1)	0.275(1)	0.270(2)

[a] CH_2Cl_2 positions at 0.096(2) 0.401(1) 0.044(2) (carbon), 0.015(2) 0.370(1) 0.085(2) (chlorine), and 0.075(2) 0.455(1) 0.043(2) (chlorine).

TABLE III. Positional Parameters of **2**·$0.75C_4H_8O$

Atom[a]	x/a	y/b	z/c
Mo	0.19715(6)	0.27094(6)	0.44867(7)
Cl(1)	0.0824(2)	0.2514(3)	0.3648(3)
Cl(2)	0.1210(2)	0.2855(2)	0.5770(2)
Cl(3)	0.3162(2)	0.2902(2)	0.5224(2)
P(1)	0.2109(2)	0.1254(2)	0.4628(3)
P(2)	0.2651(2)	0.2527(3)	0.3115(2)
P(3)	0.1861(3)	0.4143(2)	0.4210(3)
C(1)	0.1395(7)	0.0828(7)	0.5338(9)
C(2)	0.3015(7)	0.0921(7)	0.5035(9)
C(3)	0.1963(8)	0.0717(8)	0.3687(8)
C(4)	0.2482(9)	0.0904(8)	0.2967(9)
C(5)	0.2405(8)	0.1661(8)	0.2523(8)
C(6)	0.3696(7)	0.2499(8)	0.3164(8)
C(7)	0.2468(10)	0.3255(7)	0.2339(8)
C(8)	0.2568(10)	0.4075(10)	0.2607(10)
C(9)	0.1988(12)	0.4451(9)	0.3170(10)
C(10)	0.2466(12)	0.4711(9)	0.4776(11)
C(11)	0.0949(10)	0.4538(9)	0.4443(15)

[a] Atomic positions representing the THF ring disorder about $\bar{4}$ at $\frac{1}{2}0\frac{1}{4}$ were identified at 0.483(3) 0.922(3) 0.292(3) (s.o.f. 0.25), 0.528(2) 0.946(2) 0.270(3) (s.o.f. 0.50), 0.545(3) 0.020(3) 0.297(3) (s.o.f. 0.25), and 0.483(3) 0.021(3) 0.330(3) (s.o.f. 0.25); atomic coordinates describing the THF disorder about the twofold rotation axis $\frac{1}{2}\frac{1}{2}z$ were refined to 0.478(2) 0.451(2) 0.381(2) (s.o.f. 0.50), 0.450(2) 0.534(2) 0.333(2) (s.o.f. 1.0), 0.510(2) 0.564(2) 0.298(2) (s.o.f. 0.50), and 0.540(2) 0.508(3) 0.254(2) (s.o.f. 0.50). Carbon scattering factors were used in each case.

reduction of **2**·$0.75OC_4H_8$ in the presence of PMe_3 or PMe_2Ph, in THF under nitrogen atmosphere, gave the yellow chloro complexes $MoCl_2[MeP(CH_2CH_2CH_2PMe_2)_2](PMe_3)$ (**3**) and $MoCl_2[MeP(CH_2CH_2CH_2PMe_2)_2](PMe_2Ph)$ (**4**), respectively. The outcome of the Na/Hg reduction of compound **2** thus presents a further example of the subtleties involved in the synthesis of transition metal dinitrogen complexes by single-step reactions of potentially suitable precursors with reductants under nitrogen. A possible explanation for the change in the reduction behaviour, observed on passing from $MoCl_3[PhP(CH_2CH_2CH_2PPh_2)_2]$ to $MoCl_3[MeP(CH_2CH_2CH_2PMe_2)_2]$, may be put forward in terms of the enhanced basicity of the methylated chelate phosphine: compared to its phenylated analogue, the $MeP(CH_2CH_2CH_2PMe_2)_2$ ligand can provide increased electron density at the metal centre, which in turn will stabilize medium oxidation numbers, such as Mo(II), at the expense of low oxidation stages, such as Mo(0). Apparently, the difficulties encountered in the preparation of the N_2 complexes $Mo(N_2)_2[MeP(CH_2CH_2CH_2PMe_2)_2](PR_3)$ are similar to those which were met by Carmona and co-workers during their synthesis of the related trimethylphosphine derivative $Mo(N_2)_2(PMe_3)_4$ [13, 14].

Electrochemistry

For convenience, a scheme summarizing the various electrochemical and chemical transformations observed during the cyclic voltammetric study of complex **2** is given prior to discussion (Scheme 1).

The cyclic voltammogram obtained for THF solutions of pure complex **2** is depicted in Fig. 1a. The compound is found to undergo a quasi-reversible

TABLE IV. Positional Parameters of **3**·0.5OCH$_3$OH

Atom[a]	*x/a*	*y/b*	*z/c*
Mo	0.5191(2)	0.2548(2)	0.0000
P(1)	0.5029(6)	0.1629(6)	−0.1581(6)
P(2)	0.3608(5)	0.2065(6)	0.0308(6)
P(3)	0.5217(6)	0.3651(6)	0.1475(6)
P(4)	0.6834(6)	0.2910(6)	−0.0253(6)
Cl(1)	0.5704(5)	0.0776(6)	0.0750(6)
Cl(2)	0.4701(6)	0.4313(6)	−0.0746(6)
C(1)	0.526(3)	0.012(3)	−0.163(3)
C(2)	0.565(3)	0.222(3)	−0.257(3)
C(3)	0.396(2)	0.170(3)	−0.209(2)
C(4)	0.315(3)	0.122(3)	−0.150(3)
C(5)	0.283(3)	0.202(3)	−0.068(3)
C(6)	0.337(2)	0.069(3)	0.084(3)
C(7)	0.297(3)	0.299(4)	0.099(3)
C(8)	0.337(3)	0.336(4)	0.194(3)
C(9)	0.412(2)	0.419(3)	0.190(3)
C(10)	0.584(3)	0.500(3)	0.153(3)
C(11)	0.564(4)	0.289(4)	0.254(3)
C(12)	0.744(3)	0.179(3)	−0.091(3)
C(13)	0.714(2)	0.421(3)	−0.084(3)
C(14)	0.759(3)	0.292(4)	0.076(3)

[a] Fractional coordinates describing the disordered solvent molecule are 0.459(3) 0.243(5) 0.495(7) (oxygen; s.o.f. 0.50), 0.519(6) 0.151(6) 0.513(8) (carbon; s.o.f. 0.25), and 0.537(5) 0.315(7) 0.486(9) (carbon; s.o.f. 0.25).

reduction step (peak a) at a peak potential of −1.64 V to give the anion 2^-. The decrease in anodic peak height observed upon re-oxidation (peak b) shows scan rate dependence which is indicative of a chemical reaction following the electrochemical conversion of 2 into 2^-. This consecutive chemical transformation of the reduced species is tentatively interpreted as a substitution of one of the chloro ligands of 2^- by a THF donor molecule, since a comparable secondary ligand exchange process was observed during the electrochemical reduction and re-oxidation of 2 in the presence of donors different from THF, such as PMe$_3$.

The prominent features of the cyclic voltammogram measured upon addition of the phosphine were, first, a considerable decrease of the ratio of the anodic and cathodic peak heights b and a and, second, the appearance of an additional anodic peak c at −0.65 V (Fig. 1a), which developed after completion of the first cathodic scan and re-oxidation. As is shown in Fig. 1b, the anodic peak c was also observed in the cyclic voltammogram obtained for a sample of authentic $MoCl_2[MeP(CH_2CH_2CH_2PMe_2)_2]$ (complex 3). Hence the electrode process represented by c in the voltammogram of the *in situ* reaction illustrated in Fig. 1a is readily assigned to the redox couple $3/3^+$, the reduced component of which must have been formed by Cl^-/PMe_3 replace-

TABLE V. Positional Parameters of **4**

Atom	*x/a*	*y/b*	*z/c*
Mo(1)	0.24741(10)	0.35890(7)	0.14128(7)
Cl(11)	0.2540(3)	0.4743(2)	0.0821(2)
Cl(12)	0.2357(4)	0.2428(2)	0.2007(2)
P(11)	0.3513(4)	0.2896(2)	0.0605(2)
P(12)	0.1026(4)	0.3351(3)	0.0790(3)
P(13)	0.1306(4)	0.4099(3)	0.2265(2)
P(14)	0.3924(3)	0.3896(3)	0.2021(2)
C(101)	0.3958(15)	0.3400(10)	−0.0157(8)
C(102)	0.4646(14)	0.2363(9)	0.0864(9)
C(103)	0.2939(13)	0.2146(8)	0.0253(8)
C(104)	0.1964(15)	0.2375(11)	−0.0100(9)
C(105)	0.1084(15)	0.2490(9)	0.0361(9)
C(106)	0.0699(16)	0.4031(10)	0.0105(10)
C(107)	−0.0205(14)	0.3256(11)	0.1233(12)
C(108)	−0.0487(13)	0.3849(13)	0.1691(12)
C(109)	0.0033(13)	0.3773(10)	0.2319(10)
C(110)	0.1004(12)	0.5062(8)	0.2197(9)
C(111)	0.1569(14)	0.3926(11)	0.3129(8)
C(112)	0.4208(13)	0.3296(10)	0.2732(8)
C(113)	0.3830(12)	0.4792(9)	0.2410(9)
C(114)	0.5128(12)	0.3962(9)	0.1589(8)
C(115)	0.5125(12)	0.4462(9)	0.1045(8)
C(116)	0.6078(18)	0.4499(11)	0.0671(10)
C(117)	0.6912(16)	0.4056(13)	0.0883(13)
C(118)	0.6877(18)	0.3587(12)	0.1424(12)
C(119)	0.5957(15)	0.3536(10)	0.1822(10)
Mo(2)	0.25710(11)	0.85274(7)	0.12729(7)
Cl(21)	0.4261(3)	0.8425(2)	0.0842(2)
Cl(22)	0.0886(3)	0.8586(3)	0.1729(2)
P(21)	0.2504(4)	0.9827(2)	0.1489(2)
P(22)	0.3173(4)	0.8282(3)	0.2389(2)
P(23)	0.2451(4)	0.7211(2)	0.1202(2)
P(24)	0.2028(4)	0.8763(2)	0.0127(2)
C(201)	0.3664(12)	1.0288(8)	0.1310(8)
C(202)	0.1546(13)	1.0444(8)	0.1076(9)
C(203)	0.2170(14)	1.0058(8)	0.2342(8)
C(204)	0.2881(14)	0.9688(10)	0.2855(8)
C(205)	0.2664(15)	0.8875(10)	0.3033(8)
C(206)	0.4558(14)	0.8273(10)	0.2469(9)
C(207)	0.2940(16)	0.7446(9)	0.2876(8)
C(208)	0.3204(16)	0.6773(9)	0.2434(9)
C(209)	0.2354(15)	0.6677(8)	0.1987(8)
C(210)	0.3487(12)	0.6712(8)	0.0744(8)
C(211)	0.1349(12)	0.6914(8)	0.0816(9)
C(212)	0.0665(12)	0.8800(9)	0.0050(9)
C(213)	0.2478(13)	0.8089(8)	−0.0472(7)
C(214)	0.2360(15)	0.9569(8)	−0.0352(7)
C(215)	0.3328(14)	0.9735(9)	−0.0326(8)
C(216)	0.3614(14)	1.0345(11)	−0.0700(8)
C(217)	0.2944(18)	1.0795(11)	−0.1068(11)
C(218)	0.2006(20)	1.0617(10)	−0.1088(9)
C(219)	0.1639(14)	1.0004(9)	−0.0715(8)
Mo(3)	0.27050(10)	0.87113(7)	0.62901(7)
Cl(31)	0.2345(3)	0.9878(2)	0.5747(2)
Cl(32)	0.3123(4)	0.7558(2)	0.6851(2)
P(31)	0.3721(3)	0.9212(2)	0.7111(2)

(continued)

TABLE V. *(continued)*

Atom	*x/a*	*y/b*	*z/c*
P(32)	0.4193(4)	0.8509(3)	0.5587(3)
P(33)	0.1854(4)	0.8018(2)	0.5506(2)
P(34)	0.1169(3)	0.8978(2)	0.6984(2)
C(301)	0.3725(13)	1.0193(8)	0.7108(9)
C(302)	0.3504(13)	0.8987(10)	0.7981(7)
C(303)	0.5049(13)	0.8916(11)	0.7085(10)
C(304)	0.5491(15)	0.9079(13)	0.6439(12)
C(305)	0.5433(14)	0.8494(13)	0.5937(11)
C(306)	0.4313(16)	0.9175(10)	0.4905(9)
C(307)	0.4430(14)	0.7672(10)	0.5145(9)
C(308)	0.3547(13)	0.7551(10)	0.4718(9)
C(309)	0.2663(12)	0.7290(8)	0.5108(8)
C(310)	0.1308(14)	0.8527(9)	0.4772(8)
C(311)	0.0861(12)	0.7454(8)	0.5827(9)
C(312)	0.1014(12)	0.9860(9)	0.7354(8)
C(313)	0.1031(12)	0.8345(10)	0.7715(8)
C(314)	−0.0072(11)	0.8998(9)	0.6583(8)
C(315)	−0.0767(13)	0.8506(9)	0.6805(9)
C(316)	−0.1652(13)	0.8572(10)	0.6445(10)
C(317)	−0.1801(13)	0.9018(11)	0.5918(10)
C(318)	−0.1056(15)	0.9488(10)	0.5712(9)
C(319)	−0.0228(13)	0.9497(8)	0.6057(8)
Mo(4)	0.23713(11)	0.36783(7)	0.64380(7)
Cl(41)	0.0751(3)	0.4315(2)	0.6506(2)
Cl(42)	0.4017(4)	0.3054(3)	0.6386(3)
P(41)	0.2239(4)	0.3333(3)	0.5294(2)
P(42)	0.1636(5)	0.2546(3)	0.6775(3)
P(43)	0.2675(4)	0.3821(3)	0.7607(2)
P(44)	0.2964(4)	0.4884(3)	0.6112(2)
C(401)	0.1041(12)	0.3588(10)	0.4889(7)
C(402)	0.3155(12)	0.3616(9)	0.4674(7)
C(403)	0.2446(15)	0.2351(9)	0.5149(9)
C(404)	0.1583(20)	0.1929(10)	0.5528(9)
C(405)	0.1870(18)	0.1779(9)	0.6254(11)
C(406)	0.0269(17)	0.2654(11)	0.6865(12)
C(407)	0.1898(19)	0.2073(10)	0.7548(8)
C(408)	0.1866(21)	0.2596(11)	0.8138(10)
C(409)	0.2782(17)	0.3017(11)	0.8153(9)
C(410)	0.1766(15)	0.4380(10)	0.8060(8)
C(411)	0.3856(15)	0.4160(13)	0.7828(9)
C(412)	0.4339(12)	0.4937(11)	0.6139(10)
C(413)	0.2468(16)	0.5637(8)	0.6640(8)
C(414)	0.2691(14)	0.5290(8)	0.5280(8)
C(415)	0.1644(15)	0.5355(9)	0.5143(9)
C(416)	0.1405(15)	0.5610(9)	0.4513(10)
C(417)	0.2163(20)	0.5767(10)	0.4046(10)
C(418)	0.3120(17)	0.5720(10)	0.4198(9)
C(419)	0.3396(15)	0.5451(9)	0.4822(10)

ment at the primary reduction product 2^- (*cf.* Scheme 1).

The oxidation of pure complex 3 at −0.65 V corresponds to a nearly reversible electron transfer (see peaks c and d in Fig. 1b). In sharp contrast, the redox couple $3/3^+$ is highly irreversible when generated *in situ* from 2^- by Cl^-/PMe_3 exchange (Fig. 1a). The cationic species 3^+ was hence suggested to be strongly inclined to rapidly undergo resubstitution of neutral PMe_3 by the small amounts of chloride anion released during the displacement from 2^-, thus restoring the neutral Mo(III) complex 2. Consistently, addition of trace quantities of Et_4NCl to the THF solution of pure 3 rendered the oxidation step c totally irreversible (Fig. 1b; dashed voltammogram). A similar situation has previously been observed by Rohde and tom Dieck for the ruthenium derivative Ru(DAD)-$(CO)_2(PPh_3)$, where DAD = i-PrN=CHCH=NPr-i: this latter complex, which is reversibly oxidized in solutions of the pure compound, likewise shows irreversible redox behaviour when formed from reduced $[Ru(DAD)(CO)_2I_2]^-$ by release of iodide and I^-/PPh_3 replacement [15].

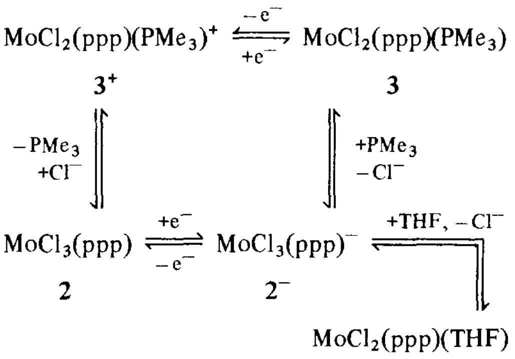

Scheme 1. Electrochemical and chemical reactions of 2 occurring in THF in the absence and presence of PMe_3; ppp = $MeP(CH_2CH_2CH_2PMe_2)_2$.

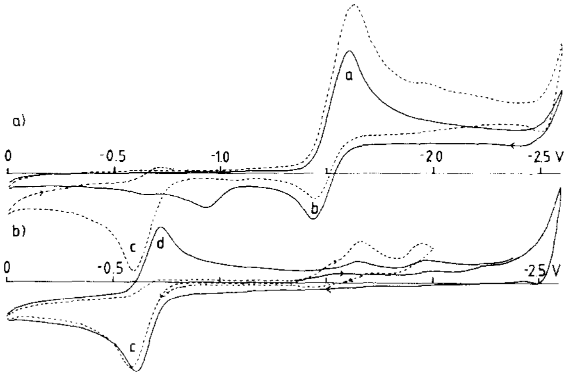

Fig. 1. (a) Cyclic voltammograms of 2 (100 mV/s); ——: pure complex; - - - -: with added PMe_3. (b) Cyclic voltammograms of 3 (100 mV/s); ——: pure complex; – – – –: in the presence of Et_4NCl.

The voltammetric behaviour of the $PhP(CH_2CH_2CH_2PPh_2)_2$ substituted complex 1 was essentially similar to that of its methylated analogue 2, reduction of 1 to 1^- occurring at a peak potential of −1.44 V. In the presence of added PPh_2Me, however, a further (irreversible) reduction step was detected at −2.40 V, which was attributed to the redox couple $MoCl_2[PhP(CH_2CH_2CH_2PPh_2)_2](PPh_2Me)/[MoCl_2[PhP(CH_2CH_2CH_2PPh_2)_2](PPh_2Me)]^-$. The observation of an additional low-potential cathodic peak for the system $1/PPh_2Me$ corresponds to our previous finding that compound 1 can easily be reduced to Mo(0) complexes by employing chemical reductants such as sodium amalgam [2]. On the other hand, the voltammetric behaviour of complex 2 in the presence of added PMe_3, which does not indicate any further reduction of the *in situ* species 2^- or 3, at potentials >*ca.* −2.50 V (Fig. 1a), compares well with the finding that 2 cannot be converted to the metal(0) state by amalgam reduction.

Structural Characterization of 1 and 2

The structures of the two trichloro molybdenum(III) complexes are shown in Figs. 2 and 3. The coordination environment of the central metal of both compounds is approximately octahedral, the ligands having the meridional arrangement.

The same geometry has also been observed in other Mo(III) species of the MoX_3L_3 type, e.g. $MoCl_3(NC_5H_5)_3$ [16], $MoBr_3(NC_5H_4Me\text{-}4)_3$ [17], $MoI_3(PMe_2Ph)_2(OPMe_2Ph)$ [18], and $MoI_3(OC_4H_8)_3$ [19]. The Mo–Cl distances (238.2(8)–243.9(8) pm in 1 and 239.6–244.3(3) pm in 2) are close to those found for similar chloro derivatives of Mo(III), such as $MoCl_3(NC_5H_5)_3$ (242.3(5)–243.7(5) pm [16]), $[MoCl_2(Me_2PCH_2CH_2PMe_2)_2]^+$ (240.1(2) and 240.7(2) pm [20]), $[MoCl_4(OC_4H_8)_2]^-$ (242.1(9)–244.1(8) pm [21]), and $MoCl_6^{3-}$ (average value 244 pm [22]).

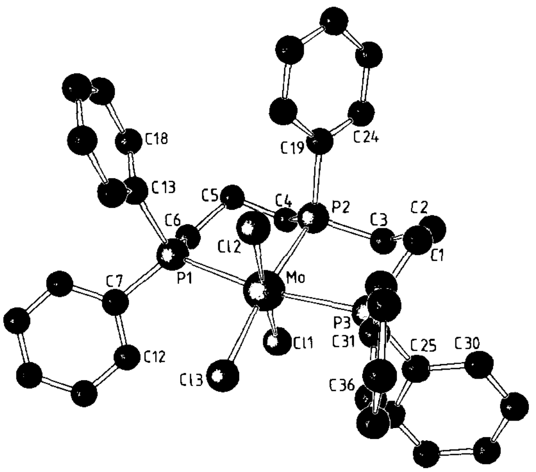

Fig. 2. Molecular arrangement and numbering scheme of the non-hydrogen atoms of 1. Selected bond lengths (pm) and angles (°) are: Cl1–Mo, 243.9(8); Cl2–Mo, 239.6(9); Cl3–Mo, 238.2(8); P1–Mo, 259.8(8); P2–Mo, 253.0(9); P3–Mo, 255.5(8). Cl2–Mo–Cl1, 177.0(3); Cl3–Mo–Cl1, 90.4(3); Cl3–Mo–Cl2, 92.5(3); P1–Mo–Cl1, 86.7(3); P1–Mo–Cl2, 93.8(3); P1–Mo–Cl3, 98.8(3); P2–Mo–Cl1, 82.1(3); P2–Mo–Cl2, 94.9(3); P2–Mo–Cl3, 171.1(3); P2–Mo–P1, 85.7(3); P3–Mo–Cl1, 96.5(3); P3–Mo–Cl2, 82.6(3); P3–Mo–Cl3, 90.4(3); P3–Mo–P1, 170.2(3); P3–Mo–P2, 85.6(3).

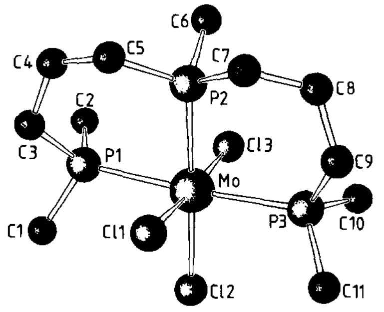

Fig. 3. The structure of 2. Important interatomic distances (pm) and angles (°) are: Cl1–Mo, 241.9(3); Cl2–Mo, 244.3(3); Cl3–Mo, 239.6(3); P1–Mo, 254.5(3); P2–Mo, 249.8(3); P3–Mo, 253.1(4). Cl2–Mo–Cl1, 91.7(1); Cl3–Mo–Cl1, 175.8(1); Cl3–Mo–Cl2, 92.5(1); P1–Mo–Cl1, 89.2(1); P1–Mo–Cl2, 94.5(1); P1–Mo–Cl3, 90.8(1); P2–Mo–Cl1, 83.6(1); P2–Mo–Cl2, 175.3(1); P2–Mo–Cl3, 92.2(1); P2–Mo–P1, 84.7(1); P3–Mo–Cl1, 88.8(1); P3–Mo–Cl2, 90.2(1); P3–Mo–Cl3, 90.8(1); P3–Mo–P1, 175.0(1); P3–Mo–P2, 90.5(1).

The unusual scattering of the metal-to-ligand bond lengths observed for 1 (239.6(9) and 243.9(8) pm in *trans*-Cl2–Mo–Cl1 *versus* 238.2(8) pm for Cl3 *trans* to Mo–P2 as well as 255.5(8) and 259.8(8) pm in *trans*-P3–Mo–P1 *versus* 253.0(8) pm for P2–Mo *trans* to Cl3–Mo) may in part be ascribed to the limited accuracy of the structure determination. On the other hand, these variations in bond lengths also appear to reflect a certain degree of spatial interference between the chloro ligands and the phenyl rings of the chelate phosphine, since there are several comparatively short non-bonding chlorine-to-*ortho*-

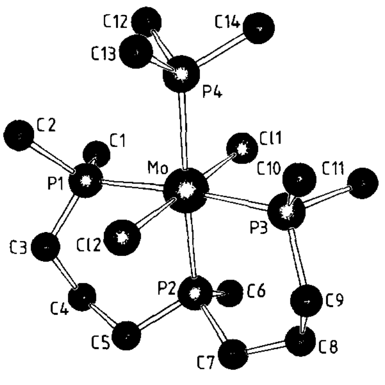

Fig. 4. Molecular structure of 3. Important interatomic distances (pm) and angles (°) are: Cl1–Mo, 245.5(6); Cl2–Mo, 243.4(7); P1–Mo, 252.1(8); P2–Mo, 246.8(7); P3–Mo, 247.7(8); P4–Mo, 251.2(8). Cl2–Mo–Cl1, 179.3(3); P1–Mo–Cl1, 93.7(3); P1–Mo–Cl2, 86.4(2); P2–Mo–Cl1, 91.5(2); P2–Mo–Cl2, 89.1(2); P2–Mo–P1, 88.4(3); P3–Mo–Cl1, 93.4(3); P3–Mo–Cl2, 86.5(3); P3–Mo–P1, 172.4(3); P3–Mo–P2, 88.9(3); P4–Mo–Cl1, 84.4(2); P4–Mo–Cl2, 95.0(3); P4–Mo–P1, 92.0(3); P4–Mo–P2, 175.9(3); P4–Mo–P3, 91.2(3).

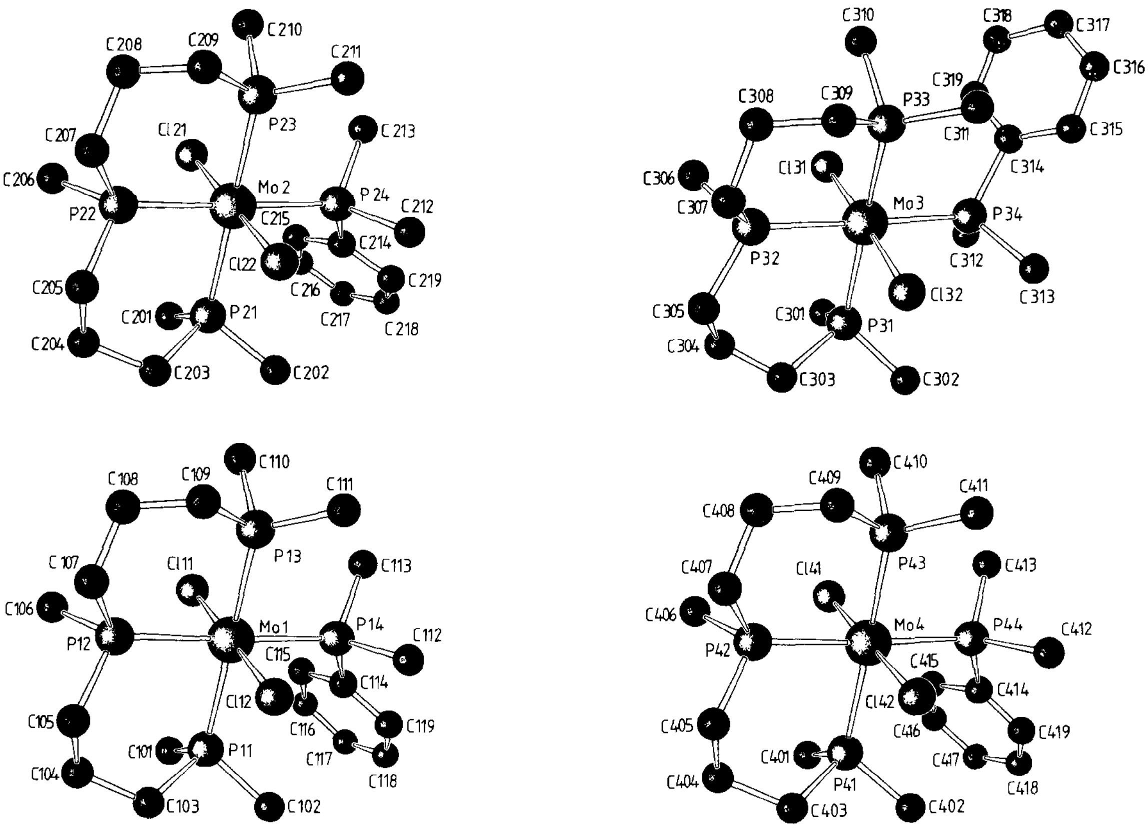

Fig. 5. The four independent molecules of **4**. Selected bond lengths (pm) and angles (°) are: Cl11–Mo1, 245.4(4); Cl12–Mo1, 247.5(5); P11–Mo1 251.2(5); P12–Mo1, 249.8(5); P13–Mo1, 252.0(5); P14–Mo1, 252.3(5). Cl12–Mo1–Cl11, 178.4(2); P11–Mo1–Cl11, 95.4(1); P11–Mo1–Cl12, 85.4(2); P12–Mo1–Cl11, 90.2(2); P12–Mo1–Cl12, 88.4(2); P12–Mo1–P11, 87.5(2); P13–Mo1–Cl11, 92.8(1); P13–Mo1–Cl12, 86.4(2); P13–Mo1–P11, 170.7(2); P13–Mo1–P12, 88.0(2); P14–Mo1–Cl11, 86.9(2); P14–Mo1–Cl12, 94.4(2); P14–Mo1–P11, 93.5(2); P14–Mo1–P12, 177.0(2); P14–Mo1–P13, 91.4(2). C21–Mo2, 245.7(5); Cl22–Mo2, 246.9(5); P21–Mo2, 251.6(5); P22–Mo2, 249.1(5); P23–Mo2, 252.4(5); P24–Mo2, 251.9(5). Cl22–Mo2–Cl21, 177.8(2); P21–Mo2–Cl21, 96.1(2); P21–Mo2–Cl22, 85.6(2); P22–Mo2–Cl21, 90.1(2); P22–Mo2–Cl22, 88.5(2); P22–Mo2–P21, 87.2(2); P23–Mo2–Cl21, 91.6(2); P23–Mo2–Cl22, 86.6(2); P23–Mo2–P21, 171.1(2); P23–Mo2–P22, 88.5(2); P24–Mo2–Cl21, 87.7(2); P24–Mo2–Cl22, 93.6(2); P24–Mo2–P21, 93.4(2); P24–Mo2–P22, 177.8(2); P24–Mo2–P23, 91.2(2). Cl31–Mo3, 244.1(4); Cl32–Mo3, 244.6(4); P31–Mo3, 251.5(5); P32–Mo3, 248.6(5); P33–Mo3, 252.5(5); P34–Mo3, 254.4(5). Cl32–Mo3–Cl31, 177.8(2); P31–Mo3–Cl31, 92.0(2); P31–Mo3–Cl32, 85.9(2); P32–Mo3–Cl31, 90.0(2); P32–Mo3–Cl32, 89.1(2); P32–Mo3–P31, 89.3(2); P33–Mo3–Cl31, 96.6(2); P33–Mo3–Cl32, 85.4(2); P33–Mo3–P31, 170.5(2); P33–Mo3–P32, 86.7(2); P34–Mo3–Cl31, 87.3(1); P34–Mo3–Cl32, 93.6(2); P34–Mo3–P31, 90.7(2); P34–Mo3–P32, 177.3(2); P34–Mo3–P33, 93.7(2). Cl41–Mo4, 244.0(4); Cl42–Mo4, 245.9(5); P41–Mo4, 251.2(5); P42–Mo4, 250.6(6); P43–Mo4, 250.8(5); P44–Mo4, 254.1(5). Cl42–Mo4–Cl41, 178.8(2); P41–Mo4–Cl41, 95.5(2); P41–Mo4–Cl42, 85.5(2); P42–Mo4–Cl41, 89.4(2); P42–Mo4–Cl42, 91.3(2); P42–Mo4–P41, 86.8(2); P43–Mo4–Cl41, 92.7(2); P43–Mo4–Cl42, 86.3(2); P43–Mo4–P41, 170.1(2); P43–Mo4–P42, 87.8(2); P44–Mo4–Cl41, 85.4(2); P44–Mo4–Cl42, 93.9(2); P44–Mo4–P41, 94.1(2); P44–Mo4–P42, 174.8(2); P44–Mo4–P43, 92.1(2).

carbon distances, e.g Cl2...C14, 328 pm, Cl2...C20, 341 pm, and Cl2...C31, 337 pm.

Due to the sterically less demanding nature of the completely methylated tris(tertiary) ligand $MeP(CH_2CH_2CH_2PMe_2)_2$, repulsive interactions should not exert a pronounced influence on the Mo–Cl and Mo–P bond lengths of **2**. According to that, the Mo–Cl distances (239.6(3) and 241.9(3) pm in *trans*-Cl3–Mo–Cl1 *versus* 244.3(3) pm for Cl2–Mo *trans* to Mo–P2) as well as the Mo–P bond lengths (253.1(4) and 254.5(3) pm in *trans*-P3–Mo–P1 *versus* 249.8(3) pm for P2–Mo *trans* to Cl2–Mo) exhibit the usual *trans* compensating features which are readily interpreted in terms of the different *trans* bond weakening capabilities of Cl and P donor ligands. The metal-to-ligand distances observed for both the *trans*-Cl–Mo–Cl and P–Mo–P moieties of **2** compare favourably with those of the cation *trans*-$[MoCl_2(Me_2PCH_2CH_2PMe_2)_2]^+$ for which Mo–Cl lengths of 240.1(2) and 240.7(2) ppm and *d*(Mo–P) values in the range 252.3(2)–254.8(2) pm have been reported recently [20].

Molecular Structures of 3 and 4

The molecular model resulting for **3** is depicted in Fig. 4. The structure analysis performed on **4** revealed the presence of four crystallographically independent molecules in the asymmetric unit of a triclinic cell. In three molecules, the orientation of the Me_2PPh ligand relative to the bridging MeP group of the chelate phosphine is equivalent in that the phenyl and methyl substituents in question point into opposite directions; the fourth molecule can be looked upon as a Me_2PPh rotamer containing the central methyl group of the chelate ligand and the Me_2PPh phenyl substituent oriented into one and the same half of the coordination sphere (see Fig. 5).

The *trans* arrangement of the halo ligands of **3** and **4** has previously been observed in related complexes exhibiting molecular dimensions similar to those listed in the captions to Figs. 4 and 5. Representative examples include: $MoCl_2(PMe_3)_4$ (Mo–Cl, 242.0(6) pm; Mo–P, 249.6(3) pm [14]), $MoCl_2(PMe_2Ph)_4$ (Mo–Cl, 243.8(1) and 244.9(1) pm; Mo–P, 251.9(1)–255.4(1) pm [23]), and $MoCl_2(Me_2PCH_2CH_2PMe_2)_2$ (Mo–Cl, 243.5(1) and 244.3(1) pm; Mo–P, 246.0(1)–246.4(1) pm [20]).

On comparing the *trans*-Me_2P–Mo–PMe_2 and *trans*-Cl–Mo–Cl bond lengths of **3** (247.7(8) and 252.1(8) pm for Mo–PMe_2; 243.4(7) and 245.5(6) pm for Mo–Cl) with those measured for the molybdenum(III) complex **2** (253.1(4) and 254.5(3) pm in *trans*-Me_2P–Mo–PMe_2; 239.6(3) and 241.9(3) pm in *trans*-Cl–Mo–Cl), it is noted that the average Mo–P distance increases on changing from Mo(II) to Mo(III) while the average Mo–Cl distance decreases. The same trends in Mo–P and Mo–Cl bond lengths of Mo(II) and Mo(III) complexes have also been reported for $MoCl_2(Me_2PCH_2CH_2PMe_2)_2$ and $[MoCl_2(Me_2PCH_2CH_2PMe_2)_2]^+$; they are most conveniently discussed in terms of the different hardnesses of the Lewis acids Mo(II) and Mo(III) leading to a tighther bonding of the harder (softer) Lewis base ligand to the Mo(III) (Mo(II)) metal centre [21].

Supplementary Material

Further details including tables of thermal parameters and calculated hydrogen positions as well as F_o/F_c listings are available from the Fachinformationszentrum Energie, Physik, Mathematik GmbH (cooperating with the Cambridge Crystallographic Data Centre), D-7514 Eggenstein-Leopoldshafen 2, F.R.G. Any request should be accompanied by the registration number CSD-52567 as well as by the full literature citation for this communication.

Acknowledgements

We gratefully acknowledge financial support by the Fonds der Chemischen Industrie and by the Deutsche Forschungsgemeinschaft. The electrochemical studies were carried out in cooperation with Prof. Dr H. tom Dieck and Dipl.-Chem. W. Rohde, to whom we express our thanks for fruitful discussion and helpful assistance.

References

1 M. Antberg, K.-M. Frosin and L. Dahlenburg, *J. Organomet. Chem., 338,* 319 (1988).
2 L. Dahlenburg and B. Pietsch, *Z. Naturforsch., Teil B, 41,* 70 (1986).
3 B. Pietsch and L. Dahlenburg, *Acta Crystallogr., Sect. C, 42,* 995 (1986).
4 M. Antberg, C. Prengel and L. Dahlenburg, *Inorg. Chem., 23,* 4170 (1984).
5 R. Alvarez, E. Carmona, M. L. Poveda and R. Sanchez-Delgado, *J. Am. Chem. Soc., 106,* 2731 (1984).
6 R. Alvarez, E. Carmona, E. Gutierrez-Puebla, J. M. Marin, A. Monge and M. L. Poveda, *J. Chem. Soc., Chem. Commun.,* 1327 (1984).
7 R. Alvarez, E. Carmona, D. J. Cole-Hamilton, A. Galindo, E. Gutierrez-Puebla, A. Monge, M. L. Poveda and C. Ruiz, *J. Am. Chem. Soc., 107,* 5529 (1985).
8 M. Brookhart, K. Cox, F. G. N. Cloke, J. C. Green, M. L. H. Green, P. M. Hare, J. Bashkin, A. E. Derome and P. D. Grebenik, *J. Chem. Soc., Dalton Trans.,* 423 (1985).
9 J. R. Dilworth and R. L. Richards, *Inorg. Synth., 20,* 119 (1980).
10 G. M. Sheldrick, 'SHELXS-84', computer programs for crystal structure solution, Göttingen, 1984.
11 G. M. Sheldrick, 'SHELX-76', program for crystal structure determination, Cambridge, 1976.
12 E. Keller, 'SCHAKAL', ein FORTRAN-Program für die graphische Darstellung von Molekülmodellen, Freiburg, 1981.
13 E. Carmona, J. M. Marin, M. L. Poveda, J. L. Atwood and R. D. Rogers, *J. Am. Chem. Soc., 105,* 3014 (1983).
14 E. Carmona, J. M. Marin, M. L. Poveda, J. L. Atwood and R. D. Rogers, *Polyhedron, 2,* 185 (1983).
15 W. Rohde and H. tom Dieck, *J. Organomet. Chem., 328,* 209 (1987).
16 J. V. Brencic, *Z. Anorg. Allg. Chem., 403,* 218 (1974).
17 J. V. Brencic and I. Leban, *Z. Anorg. Allg. Chem., 445,* 251 (1978).
18 F. A. Cotton and R. Poli, *Inorg. Chem., 25,* 3624 (1986).
19 F. A. Cotton and R. Poli, *Inorg. Chem., 26,* 1514 (1987).
20 L. K. Fong, J. R. Fox, B. M. Foxman and N. J. Cooper, *Inorg. Chem., 25,* 1880 (1986).
21 A. Hills, G. J. Leigh, J. Hutchinson and J. A. Zubieta, *J. Chem. Soc., Dalton Trans.,* 1069 (1985).
22 Z. Amilius, B. van Laar and H. M. Kietvald, *Acta Crystallogr., Sect. B, 25,* 400 (1969).
23 S. N. Anderson, D. L. Hughes and R. L. Richards, *Transition Met. Chem., 10,* 29 (1985).